Automatic Measurements of Cell Structures: Programing and Applications

Dimiter Prodanov[a,b,c]

[a]Neural Engineering Rehabilitation Laboratory, Catholic University of Louvain, Brussels, Belgium
[b]Department of Pharmacology, Sofia Medical University, Sofia, Bulgaria
[c]Neurosurgical Research Laboratory, Leiden University Medical Center, Leiden, Netherlands

ABSTRACT

This workshop demonstrates several imaging techniques in fluorescence microscopy together with programing techniques in writing *ImageJ* plugins. Techniques are applied in tasks of automatic identifcation and measurement of (i) synaptic boutons in cultured brain cells and of (ii) axonal profiles loaded with fluorescent tracer in frozen nerve sections. In the first part, mathematical granulometry is used to isolate potential synaptic boutons, which are then measured automatically. Using this approach, quantitative effects of different treatments of cell cultures can be measured. In the second part, channel subtraction and granulometry are used to reconstruct the relationship of myelinated fibers dimensions from a specific population with their tracer content. To relate the area occupied by the tracer within an axonal profile to the area of the corresponding fiber (axon + myelin sheath) paired sets of measurements were performed on representative images. A linear regression relationship could be established for the equivalent diameter of the fiber and the equivalent diameter of the axonal signal. This allows to reconstruct the total population of labeled fibers solely from the fluorescence measurements.

Keywords: cell culture, axon, synapse, retrograde tracing, synapsin 1, Fluoro-Gold, morphometry

1. SYNAPSE BOUTON MEASUREMENTS

To establish the dose- or time- dependence of a specific pharmacological effect often a large number of different experimental groups are needed. This rapidly increases the number of individual samples to be evaluated. Because of the high variability of the localizations of synapses on dendrites and the clustering of boutons, the stereological assumption of homogeneity of spatial distribution is violated. Therefore, complete dendritic trees are counted. To facilitate counting in cell cultures we developed a reproducible and robust method for automatic identification and morphometry of synaptic boutons.[1] The method is further illustrated with identifcation of synaptic boutons marked for *synapsin I* immuno-fluoresecence from micro-island cultures of neocortical neurons.

1.1. Imaging and Morphometric Analysis

Micro island cortical cultures were prepared from embryonic day 18 murine embryos. Cultures were stained with antibodies against a marker for dendrites, *microtubule-associated protein 2* (MAP-2), and a marker for synaptic vesicles, *synapsin I*. Cultures were analyzed on a Zeiss 510 Meta confocal microscope (Carl Zeiss, Heidelberg, Germany). A set of 57 high-resolution digital images of different cultures was recorded at a resolution of 4.45 pixels per μm. Images were acquired on 2 channels - *cyan*, comprising anti-synapsin staining and *red*, comprising anti-MAP-2 staining. In order to reduce the amount of debris, all but the area situated within 3 μm distance of any MAP-2 positive dendritic branches was blanked in the images.

Image processing and measurement steps were performed in the public domain software for image analysis *ImageJ* (NIH, Bethesda, Maryland, USA; http://rsb.info.nih.gov/ij/). The algorithm was run on the synapsin channel of every image. The identified boutons were numbered and their areas, equivalent diameters, and planar co-ordinates were measured and recorded.

Mailing address: GREN, Catholic University of Louvain, Av. Hippocrates 54, PO Box UCL-5446, B-1200 Brussels, Belgium; e-mail: dimiterpp@gmail.com

1.2. Outline of the Algorithm

The algorithm employed in the study can be outlined in the following main steps:

1. Perform granulometry of the image and compute its granulometric size density *G(d)* (Appendix A).
2. Identify the scale of interest by the pattern of the peaks in *G(d)*; select low bound $I_{low} = S \circ E_{low}$ and high bound images $I_{high} = S \circ E_{high}$, where $\circ$ denotes the opening operation and subtract the images.
3. Construct the binary "mask" using the *k-means clustering* algorithm[2] - a method that can overcome background autofluorescence of the studied cell structures more easily.
4. Delete irrelevant structures by superimposing the mask on the original image using bit-plane logical AND operation (masking). Threshold the resulting image using the integral thresholding (Appendix B).
5. Construct disjoint grains from the pixels that are above the threshold based on their 8-connected neighborhoods as implemented in *ImageJ*.
6. Enumerate and measure the grains constructed in this way. Produce derivative images where the identification numbers of the positive fibers are visible.

1.3. Results and Discussion

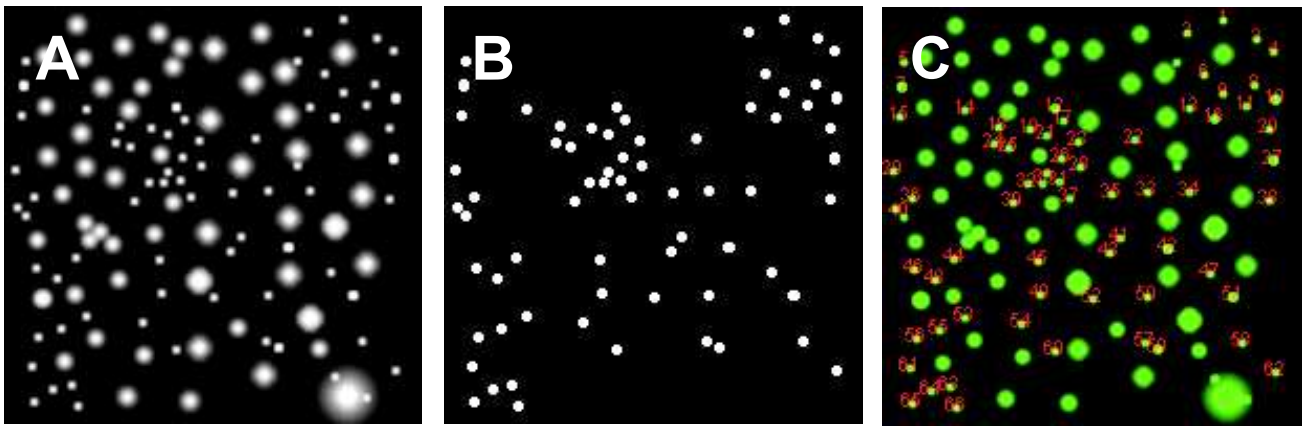

Figure 1. Granulometric filtering procedure of a synthetic image. A - Synthetic image with dimensions 200 x 200 pixels containing 127 bright grains of 5 types. The image was produced by painting randomly located circles using different brush sizes and varying degrees of fuzziness. B - the mask derived from the one of the peaks in G(d). C - Detected grains are numbered in red and overlayed onto the original image (green).

The working of the algorithm is illustrated by a synthetic image example (Fig. 1). Granulometry was performed with flat disk-shaped SEs. G(d) showed pronounced maxima that matched the brush diameters used for the drawing at d=4, 7, 10, and 13 pixels (not shown). The filtering procedure is exemplified further for the peak at d=4. A total of 66 grains comprising 3.6% of the image area was identified (red numbers, Fig. 1C).

As the fluorescent patches in the real images were round, granulometry was performed with a family of flat disk-shaped SEs ranging from d=1 to d=25 (0.2 μm - 5.6 μm). A consistent pattern could be discerned in the shape of the averaged *G(d)* - a peak region (P) in the range 0.7 - 1.6 μm, an intermediate region (shoulder - S) in the range 2.0 μm - 2.5 μm, and a decreasing region (tail - T) - from 2.9 μm on. The discerned regions were significantly different from each other ($p < 0.0001$, univariate ANOVA). The P-region corresponded to the presence of a large number of synapsin positive grains of matching sizes. The diameter range of these conformed to the size range of synaptic boutons described previously.[3] For the construction of I_{low} values of either d_{low}=3 or d_{low}=5 (i.e. P-region) were selected depending on the amount of debris in an image; d_{high}=11 was selected as a parameter for I_{high} (i.e. S-region). Based on the discrimination of dark background, auto-fluorescing cell

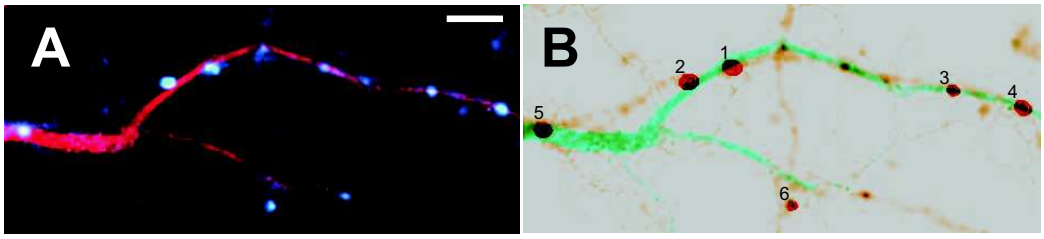

Figure 2. Illustration of the granulometric filtering technique on a real image. A - Co-localization of synapsin I (cyan) and MAP-2 (red); B - co-localization of the detected synaptic boutons (red outline) with the inverted image from A. Scale bar - 5 μm.

mass, and synapsin positive grains *three* brightness classes were used during k-means clustering. During the integral thresholding, sufficient overlap of the thresholded particles with the actual synapsin grains was typically achieved for AF=0.8 (*Area Factor*, see Appendix B). The brightest class was selected for the construction of the mask. An example outcome of the detection procedure is presented in Fig. 2B. In cultured cells, 1498 boutons were automatically detected and measured in 57 images; 90% of them had diameters between 0.95 and 2.57 μm.

An advantage of the proposed automated approach is that, apart from the number of synaptic boutons in a light microscopic image, it also allows to be measured morphological characteristics such as area, circularity, and maximal diameter. At different scales and using suitable labeling other cell structures, such as nuclei or axonal profiles, can also be identified and measured.

2. AXONAL MEASUREMENTS

Fluorescent tracers in combination with digital microscopy greatly facilitate the task of tracing axons. It is of interest to identify also the morphological type of the nerve fiber population that is traced. This can be investigated by injections of a tracer substance, such as Fluoro-Gold (FG),[4] into a muscle followed by subsequent mapping of its innervating axons on cross sections of the relevant nerve. An automated method for identification and morphometric analysis of nerve fiber populations innervating specific muscles is described here. The approach is examplified by measurements of the motor axons that innervate rat gastrocnemius muscles as identified by retrograde tracing with Fluoro-Gold.

2.1. Animals, Microscopy and Image Processing

Experiments were performed in accordance with international (EU Directive 86/609/EEC) and local laws governing the protection of experimental animals. Rats were injected in their gastrocnemius muscles with the retrograde tracer Fluoro-Gold (Fluorochrome Inc) after skin incision under general anesthesia. After 3 days of survival the rats were sacrificed and perfused transcardially with 4% Paraformaldehyde in 0.1M phosphate buffer. 14 μm cryotome sections of the nerves were inspected on Axioplan (Carl Zeiss, Sliedrecht, The Netherlands) fluorescence microscopes equipped with CCD camera. The fluorescent signal from the specimens was recorded on 2 channels. FG signal was recorded using a standard filter set for DAPI (4',6-Diamidino-2-phenylindole) detection (excitation 320 - 370 nm) (i.e. Fig. 3A). The signal from the myelin sheaths (comprising autofluorescence) was recorded using a standard filter set for FITC (Fluorescein) detection (excitation 450 - 490 nm) (Fig. 3B). Tracer-positive axonal profiles were isolated from the resulting images by means of granulometric filtering programmed as a subroutine in *ImageJ* (see Sec. 1).

2.2. Outline of the Algorithm

The algorithm employed in the study can be outlined in the following main steps:

1. Perform Separation of channels (Appednix C)
2. Perform granulometry on the resulting image and compute *G(d)*.
3. Identify the scale of interest by the pattern of the peaks in G(d); select $I_{low} = S \circ E_{low}$ and $I_{high} = S \circ E_{high}$ and subtract the images.

4. Interactively threshold the resulting image.

5. Construct disjoint grains from the pixels that are above the threshold based on their 8-connected neighborhoods as implemented in *ImageJ*.

6. Enumerate and measure the grains constructed in this way. Produce derivative images where the identification numbers of the positive fibers are visible.

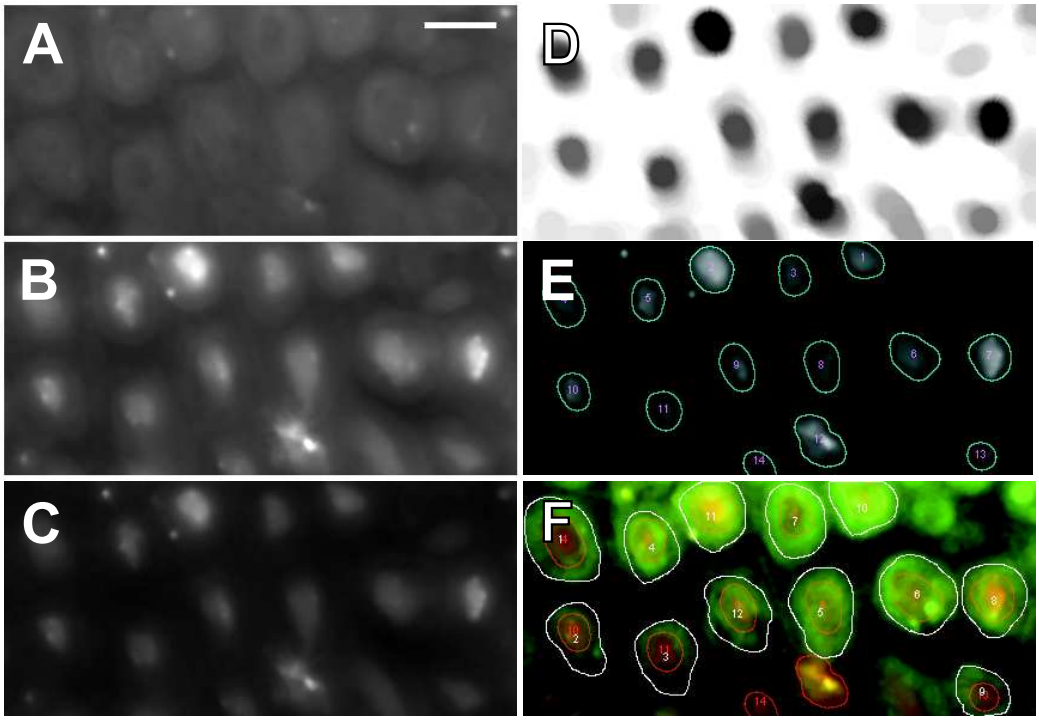

Figure 3. Illustration of the granulometric filtering technique on a real image

A - FITC channel, scale bar is 10 μm, B - FG channel. Note that the positive axons are almost entirely filled with FG. C - after recoloration the FITC channel was subtracted from the FG channel. Note the varying intensity of the residual labeling. D - granulometric filtering was applied to the C image to isolate the positive axons. The image is inverted and its brightness and contrast were adjusted to provide best observation. E - automatic measurement of the FG fluorescence. F - Manual measurements of fiber borders

2.3. Morphometry

The automatic detection and measurement of the FG-positive axons was performed in *Regions of Interest* (ROIs) (Fig. 3). Resulting images with the numbered objects were overlaid onto the original image and inspected for the accuracy of FG-positive axons (Fig. 3E). In case of sub-optimal image processing resulting in false positive or false negative axons the operator repeated the processing and measurement procedure to eliminate them. Identified FG-positive axonal profiles were automatically enumerated and outlined and their areas and corresponding diameters were calculated and recorded in a database.

Nerve fiber measurements were associated with corresponding measurements of fluorescent signal in the axon of the same fiber. The derived images (Fig. 3D) were combined with the FITC channels and the fibers that were clearly visible were manually outlined and automatically enumerated and measured (Fig. 3E). Only fibers with clearly traceable borders, which had their axons filled with tracer could be outlined manually. Thus, each fully measured fiber received 2 coupled identification numbers - one for the measurement of its FG axonal signal area and one for the measurement of its fiber area.

The relationship between the size of the labeling $d[as]$ and the size of the overall nerve fiber $d[f]$ was studied in the matched sample of fibers using (multiple) regression analysis. Probability levels of less than 0.05 were considered significant. Data are presented as means ± standard deviations.

2.4. Results and Discussion

Analysis of the *G(d)* of several representative images suggested the low bound for the filtering to be d_{low}=9 (comprising 3.7 μm) and the high bound of the filtering to be d_{high}=25 (10.2 μm). An example outcome of the filtering procedure is presented in Fig. 3D. Results are derived from 250 doubly-measured FG-positive fibers (i.e. comprising FG-positive axon surrounded by a clearly discernable myelin sheath) from a total of 10 images. Axonal signal diameters correlated with the fiber diameters in the matched sample (Pearson's $r = 0.35$, $p < 0.0001$). Regression analysis yielded the linear function

$$d[f] = 6.86 + 0.38 \cdot d[as] \tag{1}$$

The standard errors of the intercept and the slope were 0.34 μm and 0.07 respectively. Fiber population of the matched sample was reconstructed from the axonal signal using Eq. 1 and a size distribution histogram of the reconstructed fiber population was computed. In general, peaks coincided with the $A\alpha$ motor fibers.

Several factors could influence used procedure. The relationship derived in this study is strictly valid only when using similar tracing protocol, exposure time, microscope optics, and image resolution. Image resolution (e.g. magnification) affects both the automatic identification and the semi-automatic measurements. Small axons (respectively fibers) could not be imaged in sufficient detail to be outlined reliably. In addition, the bandwidth setting of the granulometric filter could influence the identification especially of the small fibers.[1] The low bound setting used during filtering was equivalent to 3.46 μm, therefore the majority of $A\gamma$ fibers could not have been reliably detected. The orientation of fibers could also affect measurements. Distortions of the shapes of the fibers caused by changes in their orientation could increase their projection area onto the plane of sectioning and consequently lead to overestimation of their equivalent diameter. Use of much shorter exposure time would heave resulted in fewer axons being detected due to underestimation of the signal intensity. In contrast, much longer exposure time would heave resulted in an increase of the overall intensity of the signal and overestimation of the amount of the labeling detected in the axons and eventually in fusing of axons (e.g. underestimation of their number).

Although imperfect for purely morphometric purposes due to the thickness of the sections introducing fuzziness of the fiber borders, the use of a fluorescent tracing protocol provids a suitable compromise between the straightforwardness and reproducibility of detection from one hand, and the accuracy of fiber dimensions reconstruction from the other. An advantage of the used approach is that it allows for a simultaneous reconstruction of the size distribution of labeled population of fibers and construction of a map of their co-ordinates from a single experiment.

ACKNOWLEDGMENTS

I would like to acknowledge W.S. Rasband from the National Institutes of Health, Bethesda, Maryland, USA for his continuous development and support of *ImageJ*.

APPENDIX A. MATHEMATICAL MORPHOLOGY

To quantify the properties of discrete sets of objects Matheron theorized empirical sieving into the formal concept of mathematical granulometry.[5] In a way similar to sieving grains, pixels comprising an image are "sieved" according to their connectivity to similar pixels imposed by a certain primitive geometric body termed *Structuring Element* (SE). Mathematically, granulometry is defined as a parameterised family of openings or closings characterized by the scale parameter d.[5] In the case of a homothetic family of SEs, granulometry can be represented by:

$$\Psi_d(S) = \bigcup_d S \circ dE \tag{2}$$

In the formula, d is the proportionality parameter of the homothety. By convention $\Psi_0(S) = S$ and for negative d *opening* is replaced by *closing*. For greyscale images, the measure of the interaction with SE is the volume $V[]$ removed by sieving. Its mapping onto the scale axis d is called granulometric size distribution:

$$\Omega(d) = V[S] - V[\Psi_d(S)] \tag{3}$$

The granulometric size density is the normalized generalized derivative of $\Omega(d)$:

$$G(d) = \frac{1}{V[S]} \frac{\partial \Omega(d)}{\partial d} \tag{4}$$

The volume of image can be estimated from its histogram H by $V[S] = \sum_{g=0}^{255} H(g) \cdot g$ and the granulometric size density by

$$G(d) = \frac{V[S \circ dE] - V[S \circ (d-1)E]}{V[S]} \tag{5}$$

Gray-level morphological operations erosion, dilation, opening and closing were implemented as a sub-routine in *ImageJ* (http://rsb.info.nih.gov/ij/plugins/gray-morphology.html).

APPENDIX B. INTEGRAL THRESHOLDING

Thresholding can be performed using $TrAF(T_{\min}, T_{\max})$, a parameterized integral threshold operator depending on the area factor parameter AF, which labels a pixel in the image if its intensity g falls between lower ($T_{\min}$) and upper threshold ($T_{\max}$) bounds constrained by the condition that the ratio between the area of the labeled pixels and the area of the non-black pixels equals AF:

$$\frac{A\left[g \in [T_{\min}\ T_{\max}]\right]}{A[g > 0]} = AF \tag{6}$$

In the formula, A[] denotes the area operator acting on the whole image. For the aims of the study, $T_{\max}$ was set to 255 while $T_{\min}$ was determined by varying its value until the condition was globally satisfied. Behavior of the threshold operator was studied previously in simulated images.[1]

APPENDIX C. SEPARATION OF CHANNELS

Due to the excitation characteristics of Fluoro-Gold its signal was absent from the FITC channel (Fig. 3 A). Therefore, it was possible to isolate the FG signal if the intensity of the FITC channel was subtracted from the intensity of the FG channel. A necessary condition to minimize the cut-off bias is that the overall resulting intensity is positive and therefore for the channels intensities should hold:

$$0 \notin Confidence[I(FG) - I(FITC)] \tag{7}$$

where $I()$ denotes channel intensity (i.e. gray value) and $Confidence$ - the confidence interval. For the optimal separation of channels images were recolored on the basis of the empirical statistics of a ROI. The following algorithm was used:

1. Calculate $K = \frac{E[I(FG)]}{P_{95}[I(FITC)]}$ where P95 denotes the 95^{th} percentile of the empirical pixel intensity distribution and E[] denotes mathematical expectation estimate.
2. Multiply the FITC channel by K: $FITC' = K \cdot FITC$
3. Subtract $FITC'$ channel from the FG channel (Fig. 3B): $I = FG - FITC'$

REFERENCES

1. D. Prodanov, J. H. Heeroma, and E. Marani, "Automatic morphometry of synaptic boutons of cultured cells using granulometric analysis of digital images," *J. Neurosci. Methods* , p. in press, 2005.
2. A. K. Jain and R. C. Dubes, *Algorithms for Clustering Data*, Prentice Hall, Englewood Cliffs, New Jersey, 1988.
3. B. Alsina, T. Vu, and S. Cohen-Cory, "Visualizing synapse formation in arborizing optic axons in vivo: dynamics and modulation by BDNF," *Nat. Neurosci.* **4**(11), pp. 1093–1101, 2001.
4. L. C. Schmued and J. H. Fallon, "Fluoro-Gold: a new fluorescent retrograde axonal tracer with numerous unique properties," *Brain Res.* **377**(1), pp. 147–154, 1986.
5. G. Matheron, *Random Sets and Integral Geometry*, Wiley series in probability and mathematical statistics, Wiley, New York, 2 ed., 1975.